

Acoustofluidics 7: The acoustic radiation force on small particles

Henrik Bruus

DOI: 10.1039/c2lc21068a

In this paper, Part 7 of the thematic tutorial series “*Acoustofluidics – exploiting ultrasonic standing waves, forces and acoustic streaming in microfluidic systems for cell and particle manipulation*”, we present the theory of the acoustic radiation force; a second-order, time-averaged effect responsible for the acoustophoretic motion of suspended, micrometre-sized particles in an ultrasound field.

1. Introduction

When an ultrasound field is imposed on a fluid containing a suspension of particles, the latter will be affected by the so-called acoustic radiation force arising from the scattering of the acoustic waves on the particle. The particle motion resulting from the acoustic radiation force is denoted acoustophoresis, and plays a key role in on-chip microparticle handling, as briefly reviewed in Part 1 of the Tutorial Series.¹

Department of Micro- and Nanotechnology,
Technical University of Denmark, DTU
Nanotech, Building 345 B, DK-2800, Kongens
Lyngby, Denmark. E-mail: Henrik.Bruus@
nanotech.dtu.dk

The studies of acoustic radiation forces on suspended particles have a long history. The analysis of incompressible particles in acoustic fields dates back to the work in 1934 by King,² while the forces on compressible particles in plane acoustic waves were calculated in 1955 by Yosioka and Kawasima.³ Their work was admirably summarized and generalized in 1962 in a short paper by Gorkov,⁴ and we follow his approach here in deriving the acoustic radiation force, filling in the details originally left out.

The theory of the radiation force relies on a perturbation expansion of the acoustic fields in the fluid. This perturbation theory is treated in detail in Part 2 of the Tutorial Series,⁵ but we summarize the main results. The ultrasound perturbations on a quiescent fluid are considered to first and second order (subscript 1 and 2, respectively) in density ρ , pressure p , and velocity \mathbf{v} ,

$$\rho = \rho_0 + \rho_1 + \rho_2, \quad (1a)$$

$$p = p_0 + c_0^2 \rho_1 + p_2, \quad (1b)$$

$$\mathbf{v} = \mathbf{v}_1 + \mathbf{v}_2, \quad (1c)$$

where c_0 is the speed of sound in the fluid, and where $p_1 = c_0^2 \rho_1$. Neglecting viscosity

in the bulk fluid,⁵ the first-order continuity and Navier–Stokes equations are

$$\partial_t \rho_1 = -\rho_0 \nabla \cdot \mathbf{v}_1, \quad (2a)$$

$$\rho_0 \partial_t \mathbf{v}_1 = -c_0^2 \nabla \rho_1. \quad (2b)$$

We assume time-harmonic fields,

$$\rho_1 = \rho_1(\mathbf{r}) e^{-i\omega t}, \quad (3a)$$

$$p_1 = p_1(\mathbf{r}) e^{-i\omega t}, \quad (3b)$$

$$\mathbf{v}_1 = \mathbf{v}_1(\mathbf{r}) e^{-i\omega t}, \quad (3c)$$

and introduce the velocity potential, ϕ_1 ,

$$\mathbf{v}_1(\mathbf{r}) = \nabla \phi_1(\mathbf{r}), \quad (4a)$$

$$p_1(\mathbf{r}) = i \rho_0 \omega \phi_1(\mathbf{r}), \quad (4b)$$

$$\rho_1(\mathbf{r}) = i \frac{\rho_0 \omega}{c_0^2} \phi_1(\mathbf{r}). \quad (4c)$$

The potential fulfils the wave equation

$$\nabla^2 \phi_1 = \frac{1}{c_0^2} \partial_t^2 \phi_1 = -\frac{\omega^2}{c_0^2} \phi_1, \quad (5)$$

which forms the starting point for the scattering theory used below to calculate the acoustic radiation force acting on the particle.

The observed acoustophoretic motion is not resolved on the μs time scale of the

Foreword

The acoustic radiation force is a key parameter in the field of acoustofluidics and is most commonly utilised in acoustic particle and cell manipulation. In this seventh paper of 23 in the *Lab on a Chip* tutorial series of Acoustofluidics, Henrik Bruus describes the theory behind the forces acting on single particles in an acoustic field, not taking into account particle–particle interactions that occur at higher particle concentrations. Starting from perturbation theory, the fundamental acoustic radiation force expression is derived and examples for theoretical validation are presented.

Andreas Lenshof – coordinator of the Acoustofluidics series

imposed MHz ultrasound wave, but is the result of the radiation force averaged over a full oscillation cycle. Thus, regarding the second-order perturbation terms, we only need to study time averages $\langle X \rangle$ over a full oscillation period τ of quantities, $X(t)$,

$$\langle X \rangle \equiv \frac{1}{\tau} \int_0^\tau dt X(t). \quad (6)$$

The time-averaged, second-order acoustic pressure $\langle p_2 \rangle$ in the inviscid bulk fluid is given by⁵

$$\nabla \langle p_2 \rangle = -\langle p_1 \partial_t \mathbf{v}_1 \rangle - \rho_0 \langle (\mathbf{v}_1 \cdot \nabla) \mathbf{v}_1 \rangle, \quad (7a)$$

$$\langle p_2 \rangle = \frac{1}{2} \kappa_0 \langle p_1^2 \rangle - \frac{1}{2} \rho_0 \langle v_1^2 \rangle, \quad (7b)$$

where in the latter equality we have used eqn (2b) and (4a) to obtain $-\langle \rho_1 \partial_t \mathbf{v}_1 \rangle = (c_0^2/2\rho_0) \nabla \langle \rho_1^2 \rangle$ and $\langle (\mathbf{v}_1 \cdot \nabla) \mathbf{v}_1 \rangle = (1/2) \nabla \langle v_1^2 \rangle$, respectively, and introduced the compressibility $\kappa_0 = 1/(\rho_0 c_0^2)$ of the fluid. We note that the physical, real-valued time average $\langle f g \rangle$ of two harmonically varying fields f and g with the complex representation eqn (3), is given by the real-part rule

$$\langle f g \rangle = \frac{1}{2} \text{Re}[f(\mathbf{r})g^*(\mathbf{r})], \quad (8)$$

where the asterisk denotes complex conjugation.

II. The acoustic radiation force

Below we calculate the acoustic radiation force on a compressible, spherical, micrometre-sized particle of radius a suspended in an inviscid fluid in an ultrasound field of wavelength λ . A small particle, *i.e.* $a \ll \lambda$, of density ρ_p and compressibility κ_p acts as a weak point-scatterer of acoustic waves, which thus can be treated by first-order

scattering theory. An incoming wave described by some given velocity potential ϕ_{in} , results in a scattered wave ϕ_{sc} propagating away from the particle. For sufficiently weak incoming and scattered waves, the total first-order acoustic field ϕ_1 is given by the sum of the two as sketched in Fig. 1(a),

$$\phi_1 = \phi_{\text{in}} + \phi_{\text{sc}}, \quad (9a)$$

$$\mathbf{v}_1 = \nabla \phi_1 = \nabla \phi_{\text{in}} + \nabla \phi_{\text{sc}}, \quad (9b)$$

$$p_1 = i\rho_0 \omega \phi_1 = i\rho_0 \omega \phi_{\text{in}} + i\rho_0 \omega \phi_{\text{sc}}. \quad (9c)$$

Once the first-order scattered field ϕ_{sc} has been determined for the given incoming first-order field ϕ_{in} , the acoustic radiation force \mathbf{F}^{rad} on the particle can be calculated as the surface integral of the time-averaged second-order pressure p_2 and momentum flux tensor $\rho_0 \langle \mathbf{v}_1 \mathbf{v}_1 \rangle$ at a fixed surface just outside the oscillating sphere, represented by the black circle and green arrows in Fig. 1(b). This follows from the general method of calculating the rate of change of the momentum applied to the inviscid fluid, see Part 1 of the Tutorial Series.¹ The expression for \mathbf{F}^{rad} becomes

$$\begin{aligned} \mathbf{F}^{\text{rad}} &= - \int_{\partial\Omega} da \left\{ \langle p_2 \rangle \mathbf{n} + \rho_0 \langle (\mathbf{n} \cdot \mathbf{v}_1) \mathbf{v}_1 \rangle \right\} \\ &= - \int_{\partial\Omega} da \left\{ \left[\frac{1}{2} \kappa_0 \langle p_1^2 \rangle - \frac{1}{2} \rho_0 \langle v_1^2 \rangle \right] \mathbf{n} \right. \\ &\quad \left. + \rho_0 \langle (\mathbf{n} \cdot \mathbf{v}_1) \mathbf{v}_1 \rangle \right\}. \quad (10) \end{aligned}$$

As there are no body forces in this problem, any fixed surface $\partial\Omega$ encompassing the sphere experiences the same

force, and given the result of the following scattering theory analysis, it is advantageous to choose a sphere of radius $r \gg \lambda$ in the far-field region, represented by the dashed circle and the red arrows in Fig. 1(b), with its centre coinciding with that of the spherical particle.

III. Scattering theory

In scattering theory, the scattered field ϕ_{sc} from a point scatterer at the centre of the coordinate system, is represented by a time-retarded multipole expansion. In the far-field region, the monopole and dipole components dominate, $\phi_{\text{sc}} \approx \phi_{\text{mp}} + \phi_{\text{dp}}$. As verified by insertion into eqn (5), these two components have the form $\phi_{\text{mp}}(\mathbf{r}, t) = b(t - r/c_0)/r$ and $\phi_{\text{dp}}(\mathbf{r}, t) = \nabla \cdot [\mathbf{B}(t - r/c_0)/r]$, where b is a scalar function and \mathbf{B} a vector function of the retarded argument $t - r/c_0$. In first-order scattering theory, ϕ_{sc} must be proportional to the incoming field ϕ_{in} . The only physically relevant scalar field is the density, $b \sim \rho_{\text{in}}$, while the only relevant vector field is the velocity, $\mathbf{B} \sim \mathbf{v}_{\text{in}}$. Here both ρ_{in} and \mathbf{v}_{in} are evaluated at the particle position with time-retarded arguments, and the far-field region ϕ_{sc} must have the form

$$\begin{aligned} \phi_{\text{sc}}(\mathbf{r}, t) &= -f_1 \frac{a^3}{3\rho_0} \frac{\partial_t \rho_{\text{in}}(t - r/c_0)}{r} \\ &\quad - f_2 \frac{a^3}{2} \nabla \cdot \left(\frac{\mathbf{v}_{\text{in}}(t - r/c_0)}{r} \right), \end{aligned} \quad (11)$$

for $r \gg \lambda$,

where the particle radius a , the unperturbed density ρ_0 , and the time derivative ∂_t are introduced to ensure the correct physical dimension of ϕ_{sc} , namely $\text{m}^2 \text{s}^{-1}$. The factors 1/3 and 1/2 are inserted for later convenience. The main goal of the calculation is to determine the dimensionless scattering coefficients f_1 and f_2 .

In the following we use a spherical coordinate system with unit vectors ($\mathbf{e}_r, \mathbf{e}_\theta, \mathbf{e}_\phi$) located at the instantaneous centre of the particle. Due to the azimuthal symmetry of the problem, the velocities have no azimuthal component, $\mathbf{v} = v_r \mathbf{e}_r + v_\theta \mathbf{e}_\theta$, and all fields depend only on r and θ . The polar axis \mathbf{e}_z points along the instantaneous direction of the incoming velocity \mathbf{v}_{in} , such that $\mathbf{v}_{\text{in}} = v_{\text{in}} \mathbf{e}_z$. By the azimuthal symmetry of the problem, the particle must also move in that direction, $\mathbf{v}_p = v_p \mathbf{e}_z$,



Henrik Bruus

Prof. Henrik Bruus received his BSc in mathematics and physics from the University of Copenhagen in 1984, and his MSc and PhD degrees in physics from the Niels Bohr Institute, University of Copenhagen in 1986 and 1990, respectively. He was post doctoral fellow at Nordic Institute of Theoretical Physics 1990–92, Yale University 1992–94 and CNRS Grenoble 1994–96. He returned to the Niels Bohr Institute as an associate professor between 1997–2001, before joining the faculty at DTU Nanotech, Technical University of Denmark in 2002. He was promoted to full professor there in 2005. He has (co)authored more than 100 peer-reviewed journal papers on condensed matter physics and microfluidics, as well as 120 peer-reviewed conference contributions and 2 monographs, the latest being “Theoretical Microfluidics”, Oxford University Press (2008).

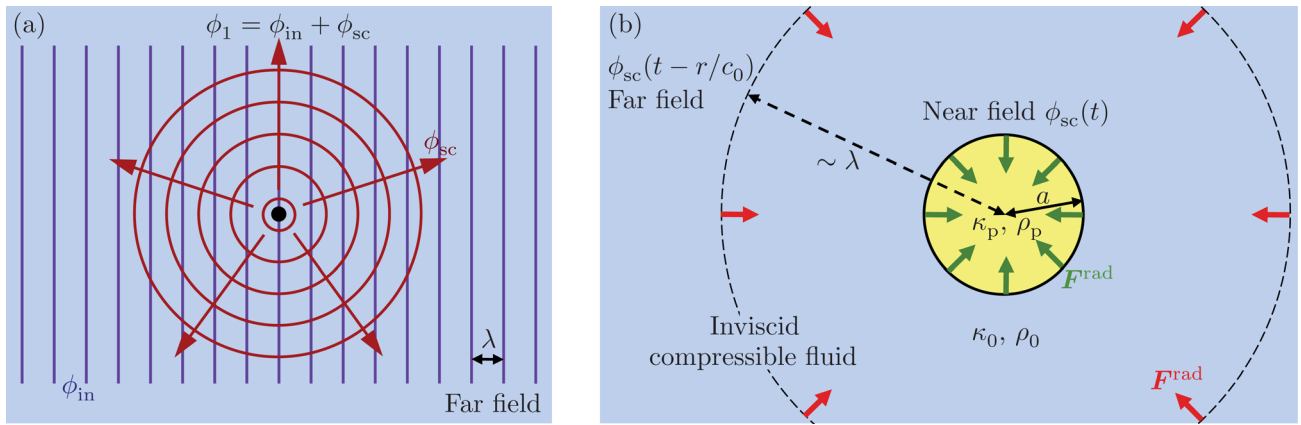


Fig. 1 (a) Sketch of the far-field region $r \gg \lambda$ of an incoming acoustic wave ϕ_{in} (blue lines) of wavelength λ scattering off a small particle (black dot) with radius $a \ll \lambda$, leading to the outgoing scattered wave ϕ_{sc} (red circles and arrows). The resulting first-order wave is $\phi_1 = \phi_{\text{in}} + \phi_{\text{sc}}$. (b) Sketch of a compressible spherical particle (yellow disk) of radius a , compressibility κ_p , and density ρ_p , surrounded by the compressible inviscid bulk fluid (light blue) of compressibility κ_0 and density ρ_0 . The fluid is divided into the near-field region for $r \ll \lambda$, with the instantaneous field $\phi_{\text{sc}}(t)$, and the far-field region with the time-retarded field $\phi_{\text{sc}}(t - r/c_0)$. The radiation force, F^{rad} (red arrows), evaluated at any surface in the far-field region (dashed circle), equals that evaluated at the surface of the sphere (green arrows).

$$v_{\text{in}} = v_{\text{in}} e_z = \cos\theta v_{\text{in}} e_r - \sin\theta v_{\text{in}} e_\theta, \quad (12a)$$

$$v_p = v_p e_z = \cos\theta v_p e_r - \sin\theta v_p e_\theta. \quad (12b)$$

A. Scattering and the radiation force

Before the values of the scattering coefficients are determined, we are able to express the radiation force F^{rad} in terms of the incoming acoustic wave evaluated at the particle position as well as the coefficients f_1 and f_2 as follows. When inserting the velocity potentials eqn (9a) and (11) into eqn (10) for F^{rad} , we obtain a sum of terms each proportional to the square of $\phi_1 = \phi_{\text{in}} + \phi_{\text{sc}}$. This results in three types of contributions: (i) squares of ϕ_{in} containing no information about the scattering and therefore yielding zero, (ii) squares of ϕ_{sc} proportional to the square of the particle volume a^6 and therefore negligible compared to (iii) the mixed products $\phi_{\text{in}}\phi_{\text{sc}}$ proportional to particle volume a^3 , and therefore the most dominant contribution to the radiation force. Keeping only these mixed terms, which physically can be interpreted as interference between the incoming and the scattered wave, and using the index notation¹ (including summation of repeated indices), the i th component of eqn (10) becomes

$$F_i^{\text{rad}} = - \int_{\partial\Omega} da n_j \left\{ \left[\frac{c_0^2}{\rho_0} \langle \rho_{\text{in}} \rho_{\text{sc}} \rangle - \rho_0 \langle v_k^{\text{in}} v_k^{\text{sc}} \rangle \right] \delta_{ij} + \rho_0 \langle v_i^{\text{in}} v_j^{\text{sc}} \rangle + \rho_0 \langle v_i^{\text{sc}} v_j^{\text{in}} \rangle \right\} \quad (13a)$$

$$= - \int_{\Omega} dr \partial_j \left\{ \left[\frac{c_0^2}{\rho_0} \langle \rho_{\text{in}} \rho_{\text{sc}} \rangle - \rho_0 \langle v_k^{\text{in}} v_k^{\text{sc}} \rangle \right] \delta_{ij} + \rho_0 \langle v_i^{\text{in}} v_j^{\text{sc}} \rangle + \rho_0 \langle v_i^{\text{sc}} v_j^{\text{in}} \rangle \right\} \quad (13b)$$

$$= - \int_{\Omega} dr \left\{ \frac{c_0^2}{\rho_0} [\langle \rho_{\text{in}} \partial_i \rho_{\text{sc}} \rangle + \langle \rho_{\text{sc}} \partial_i \rho_{\text{in}} \rangle] + \rho_0 [\langle v_i^{\text{in}} \partial_j v_j^{\text{sc}} \rangle + \langle v_i^{\text{sc}} \partial_j v_j^{\text{in}} \rangle] \right\} \quad (13c)$$

$$= - \int_{\Omega} dr \left\{ - \langle \rho_{\text{in}} \partial_i v_i^{\text{sc}} \rangle - \langle \rho_{\text{sc}} \partial_i v_i^{\text{in}} \rangle + \rho_0 \langle v_i^{\text{in}} \partial_j v_j^{\text{sc}} \rangle - \langle v_j^{\text{sc}} \partial_i \rho_{\text{in}} \rangle \right\} \quad (13d)$$

$$= - \int_{\Omega} dr \left\{ \langle v_i^{\text{in}} \partial_i \rho_{\text{sc}} \rangle + \rho_0 \langle v_j^{\text{in}} \partial_j v_i^{\text{sc}} \rangle \right\} \quad (13e)$$

$$= - \int_{\Omega} dr \rho_0 \left\langle v_i^{\text{in}} \left(\partial_j \partial_j \phi_{\text{sc}} - \frac{1}{c_0^2} \partial_i^2 \phi_{\text{sc}} \right) \right\rangle \quad (13f)$$

Here, we have used $p_1 = c_0^2 \rho_1$ in eqn (13a), Gauss's theorem in eqn (13b), exchange of indices $\partial_i v_k = \partial_k \partial_i \phi = \partial_k \partial_i \phi = \partial_k \partial_i \phi = \partial_k v_i$ to cancel terms in eqn (13c), introduction of time derivatives by the continuity equation $\partial_t \rho_1 = -\rho_0 \partial_j v_{1,j}$ and the Navier–Stokes equation $\rho_0 \partial_t v_{1,i} = -\partial_i p_1 = -c_0^2 \partial_i \rho_1$ in eqn (13d), vanishing of time-averages of total time derivatives $\langle \partial_t (\rho v_i) \rangle = 0$ or $\langle \rho \partial_t v_i \rangle = -\langle v_i \partial_t \rho \rangle$ for cancellation and rearrangement in eqn (13e), and finally reintroduction of the vector potential ϕ_{sc} in eqn (13f).

The d'Alembert wave operator $\partial_j \partial_j - (1/c_0^2) \partial_t^2$ acting on ϕ_{sc} appears in the integrand of eqn (13f), and since ϕ_{sc} is

a sum of simple monopole and dipole terms, significant simplifications are possible. Just as the Laplace operator acting on the monopole potential $\phi = q/(4\pi\epsilon_0 r)$ yields the point-charge distribution, $\partial_j^2 \phi = -(q/\epsilon_0) \delta(\mathbf{r})$, in the static case, the d'Alembert operator acting on the retarded-time monopole and dipole expressions (11) also yields delta function distributions,

$$\partial_j^2 \phi_{\text{sc}} - \frac{1}{c_0^2} \partial_t^2 \phi_{\text{sc}} = f_1 \frac{4\pi a^3}{3\rho_0} \partial_i \rho_{\text{in}} \delta(\mathbf{r}) + f_2 2\pi a^3 \nabla \cdot [\mathbf{v}_{\text{in}} \delta(\mathbf{r})], \quad (14)$$

for $r \gg \lambda$.

Now we see the great advantage of working in the far-field limit. The first term is easily integrated, when appearing in eqn (13f), but for the second term we need to get rid of the divergence operator acting on the delta function before we can evaluate the integral. This we manage by Gauss's theorem. First we note that $\nabla \cdot [\mathbf{v}(\mathbf{r}) \mathbf{u}(\mathbf{r})] = \mathbf{v} \nabla \cdot \mathbf{u} + \mathbf{u} \cdot \nabla \mathbf{v}$ for any scalar function v and vector function \mathbf{u} . Therefore, $\int_{\partial\Omega} da \mathbf{n} \cdot (\mathbf{v} \mathbf{u}) = \int_{\Omega} dr \nabla \cdot (\mathbf{v} \mathbf{u}) = \int_{\Omega} dr (\mathbf{v} \nabla \cdot \mathbf{u} + \mathbf{u} \cdot \nabla \mathbf{v})$, and we have derived the integral identity $\int_{\partial\Omega} dr \mathbf{v} \nabla \cdot \mathbf{u} = - \int_{\Omega} dr \mathbf{u} \cdot \nabla \mathbf{v} + \int_{\partial\Omega} da \mathbf{n} \cdot (\mathbf{v} \mathbf{u})$. Now, since $\mathbf{u} \propto \mathbf{v} \delta(\mathbf{r})$ we obtain in eqn (13f) a volume integral encompassing the delta function singularity, thus yielding a non-zero contribution, and a surface integral avoiding the delta function singularity thus yielding zero. Consequently, the resulting expression for F^{rad} becomes

$$\mathbf{F}^{\text{rad}} = -\frac{4\pi}{3}a^3 \langle f_1 v_{\text{in}} \partial_t \rho_{\text{in}} \rangle \quad (15a)$$

$$+ 2\pi a^3 \rho_0 \langle f_2 (\mathbf{v}_{\text{in}} \cdot \nabla) \mathbf{v}_{\text{in}} \rangle$$

$$= +\frac{4\pi}{3}a^3 \langle f_1 p_{\text{in}} \partial_t \mathbf{v}_{\text{in}} \rangle \quad (15b)$$

$$+ 2\pi a^3 \rho_0 \langle f_2 (\mathbf{v}_{\text{in}} \cdot \nabla) \mathbf{v}_{\text{in}} \rangle$$

$$= -\frac{4\pi}{3\rho_0 c_0^2} a^3 \langle f_1 p_{\text{in}} \nabla p_{\text{in}} \rangle \quad (15c)$$

$$+ 2\pi a^3 \rho_0 \langle f_2 (\mathbf{v}_{\text{in}} \cdot \nabla) \mathbf{v}_{\text{in}} \rangle$$

$$= -\text{Re}[f_1] \frac{2\pi}{3} a^3 \kappa_0 \nabla \langle v_{\text{in}}^2 \rangle \quad (15d)$$

$$+ \text{Re}[f_2] \pi a^3 \rho_0 \nabla \langle v_{\text{in}}^2 \rangle,$$

with p_{in} and v_{in} evaluated at $r = 0$.

Here we have integrated over the delta function in eqn (15a), applied the previously used rule $\langle \rho_{\text{in}} \partial_t \mathbf{v}_{\text{in}} \rangle = -\langle v_{\text{in}} \partial_t \rho_{\text{in}} \rangle$ in eqn (15b), inserted $\rho_{\text{in}} = p_{\text{in}}/c_0^2$ and $\partial_t \mathbf{v}_{\text{in}} = -\nabla p_{\text{in}}/\rho_0$ in eqn (15c), and finally pulled f_1 and f_2 outside the time averages (using eqn (8)) together with the nabla operator in eqn (15d). The final expression for the radiation force acting on a small particle ($a \ll \lambda$) is,

$$\mathbf{F}^{\text{rad}} = -\frac{4\pi}{3}a^3 \nabla \left[\frac{1}{2} \text{Re}[f_1] \kappa_0 \langle p_{\text{in}}^2 \rangle - \frac{3}{4} \text{Re}[f_2] \rho_0 \langle v_{\text{in}}^2 \rangle \right]. \quad (16)$$

Now we need to determine the coefficients f_1 and f_2 .

B. The near-field potential

As sketched in Fig. 1(b), the time-retarded argument $t - r/c_0$ of the acoustic field ϕ_1 can be replaced by the instantaneous argument t in the vicinity of the particle of radius a . The reason is that within one oscillation period $\tau = 2\pi/\omega$, the retardation time over the distances $r \simeq a$ is negligible, $r/c_0 \simeq a/c_0 \ll \lambda/c_0 = \tau$. Therefore, in the near-field region, ϕ_{in} derived in eqn (12a) and the scattering potential ϕ_{sc} of eqn (11) with its monopole and dipole term become

$$\phi_{\text{in}}(r, \theta) = v_{\text{in}} r \cos \theta, \quad (17a)$$

$$\phi_{\text{sc}}(r, \theta) = \phi_{\text{mp}}(r) + \phi_{\text{dp}}(r, \theta),$$

$$\text{for } r \ll \lambda, \quad (17b)$$

$$\phi_{\text{mp}}(r) = -f_1 \frac{a^3}{3\rho_0} \partial_t \rho_{\text{in}} \frac{1}{r}, \quad (17c)$$

$$\phi_{\text{dp}}(r, \theta) = +f_2 \frac{a^3}{2} v_{\text{in}} \frac{\cos \theta}{r^2}, \quad (17d)$$

where $\partial_t \rho_{\text{in}}$ and v_{in} are evaluated at the position of the particle, $r = 0$. In first-order scattering theory, the monopole and dipole parts of the problem do not mix: f_1 is the coefficient in the monopole scattering potential ϕ_{mp} from a stationary sphere in the incoming density wave ρ_{in} , while f_2 is the coefficient in the dipole scattering potential ϕ_{dp} from an incompressible sphere moving with velocity v_p in the incoming velocity wave v_{in} .

C. The monopole coefficient f_1

The presence of the particle gives rise to a mass rate $\partial_t m$ of scattered fluid mass given by the first-order, scattered mass flux $\rho_0 \nabla \phi_{\text{mp}}$. By integration over the surface of the sphere we obtain

$$\partial_t m = \int_{\partial\Omega} da e_r \cdot (\rho_0 \nabla \phi_{\text{mp}}) \quad (18)$$

$$= f_1 \frac{4\pi}{3} a^3 \partial_t \rho_{\text{in}}.$$

The factor $1/3$ was introduced in eqn (11) to make the particle volume $V_p = (4\pi/3)a^3$ appear here. The rate of scattered fluid mass can also be written in terms of the rate of change of the incoming density $\rho_0 + \rho_{\text{in}}$ multiplied by V_p as $\partial_t m = \partial_t [\{\rho_0 + \rho_{\text{in}}(t)\} V_p(t)]$. Expressing this through the compressibility $\kappa = -(1/V)(\partial V/\partial p)$ of the particle, κ_p , and of the fluid, $\kappa_0 = 1/(\rho_0 c_0^2)$, we obtain,

$$\partial_t m = \left[1 - \frac{\kappa_p}{\kappa_0} \right] V_p \partial_t \rho_{\text{in}}, \quad (19)$$

by using $\partial_t V_p = \partial_p V_p \partial_t p_{\text{in}} = -c_0^2 V_p \kappa_p \partial_t \rho_{\text{in}}$. Now, f_1 is obtained by equating eqn (18) and (19),

$$f_1(\tilde{\kappa}) = 1 - \tilde{\kappa}, \text{ with } \tilde{\kappa} = \frac{\kappa_p}{\kappa_0}. \quad (20)$$

D. The dipole coefficient f_2

The dipole coefficient f_2 is related to the translational motion of the particle. For an inviscid fluid, there is only a boundary condition for the radial-direction components of the particle velocity v_p of

eqn (12b) and the dipole part of the fluid velocity,

$$\mathbf{e}_r \cdot \mathbf{v}_p = \mathbf{e}_r \cdot \nabla (\phi_{\text{in}} + \phi_{\text{dp}}). \quad (21)$$

At $r = a$ we obtain $\mathbf{e}_r \cdot \nabla (\phi_{\text{in}} + \phi_{\text{dp}}) = (1 - f_2) v_{\text{in}} \cos \theta$ from eqn (17a) and (17d), whereby eqn (21) becomes

$$v_p = (1 - f_2) v_{\text{in}}. \quad (22)$$

The particle velocity v_p is also given by Newton's second law with $\partial_t v_p = -i\omega v_p$ and the dipole part $p_{\text{in}} + p_{\text{dp}}$ of the fluid pressure acting on the surface of the sphere,

$$-i \frac{4}{3} \pi a^3 \rho_p \omega v_p$$

$$= -2\pi a^2 \int_{-1}^1 d(\cos \theta) (p_{\text{in}} + p_{\text{dp}}) \cos \theta. \quad (23)$$

From eqn (9c), (17a), and (17d) we obtain

$$p_{\text{in}} + p_{\text{dp}} = i\rho_0 \omega (\phi_{\text{in}} + \phi_{\text{dp}})$$

$$= i\rho_0 \omega a \left[1 + \frac{1}{2} f_2 \right] v_{\text{in}} \cos \theta, \quad (24)$$

which together with eqn (23) leads to

$$\tilde{\rho} v_p = \left[1 + \frac{1}{2} f_2 \right] v_{\text{in}}, \text{ with } \tilde{\rho} = \frac{\rho_p}{\rho_0}. \quad (25)$$

The dipole coefficient f_2 follows from eqn (22) and (25),

$$f_2(\tilde{\rho}) = \frac{2(\tilde{\rho} - 1)}{2\tilde{\rho} + 1}. \quad (26)$$

E. The resulting radiation force

In summary, the resulting radiation force \mathbf{F}^{rad} on a small, spherical particle ($a \ll \lambda$) in an inviscid fluid is the gradient of an acoustic potential U^{rad} ,

$$\mathbf{F}^{\text{rad}} = -\nabla U^{\text{rad}}, \quad (27a)$$

$$U^{\text{rad}} = \frac{4\pi}{3} a^3 \left[f_1 \frac{1}{2} \kappa_0 \langle p_{\text{in}}^2 \rangle - f_2 \frac{3}{4} \rho_0 \langle v_{\text{in}}^2 \rangle \right], \quad (27b)$$

$$f_1(\tilde{\kappa}) = 1 - \tilde{\kappa}, \text{ with } \tilde{\kappa} = \frac{\kappa_p}{\kappa_0}, \quad (27c)$$

$$f_2(\tilde{\rho}) = \frac{2(\tilde{\rho} - 1)}{2\tilde{\rho} + 1}, \text{ with } \tilde{\rho} = \frac{\rho_p}{\rho_0}. \quad (27d)$$

IV. Standing plane wave

Our prime example of the acoustic radiation force is the 1D planar standing

$\lambda/2$ -wave, $p_1(z) = p_a \cos(kz)$, where $k = 2\pi/\lambda = \omega/c_0$ and $\lambda/2 = w$, w being the channel width, see Fig. 2. This has been realized in numerous applications in microchannel acoustophoresis.¹ Here, we analyze the radiation force resulting from such a field. The first-order, incoming, acoustic fields are given by

$$\phi_{\text{in}}(z, t) = \frac{P_a}{\rho_0 \omega} \cos(kz) \cos(\omega t) \quad (28a)$$

$$p_{\text{in}}(z, t) = p_a \cos(kz) \sin(\omega t), \quad (28b)$$

$$\rho_{\text{in}}(z, t) = \frac{P_a}{c_0^2} \cos(kz) \sin(\omega t), \quad (28c)$$

$$\mathbf{v}_{\text{in}}(z, t) = -\frac{P_a}{\rho_0 c_0} \sin(kz) \cos(\omega t) \mathbf{e}_z, \quad (28d)$$

where we have used the usual real-time representation. With these fields, the time averages needed in eqn (27) are simply $\langle \cos^2(\omega t) \rangle = \langle \sin^2(\omega t) \rangle = \frac{1}{2}$, and we arrive at the following expression for the radiation potential

$$U^{\text{rad}} = \left[\frac{f_1}{3} \cos^2(kz) - \frac{f_2}{2} \sin^2(kz) \right] \times \pi a^3 \kappa_0 p_a^2, \quad (29)$$

The radiation force is found by differentiation,

$$F_z^{\text{rad}} = -\partial_z U^{\text{rad}} = 4\pi\Phi(\tilde{\kappa}, \tilde{\rho}) k a^3 E_{\text{ac}} \sin(2kz), \quad (30a)$$

$$E_{\text{ac}} = \frac{p_a^2}{4\rho_0 c_0^2}, \quad (30b)$$

$$\Phi(\tilde{\kappa}, \tilde{\rho}) = \frac{1}{3} f_1(\tilde{\kappa}) + \frac{1}{2} f_2(\tilde{\rho}) = \frac{1}{3} \left[\frac{5\tilde{\rho} - 2}{2\tilde{\rho} + 1} - \tilde{\kappa} \right], \quad (30c)$$

where E_{ac} is the acoustic energy density and $\Phi(\tilde{\kappa}, \tilde{\rho})$ is the so-called acoustophoretic contrast factor. The factor $\sin(2kz)$ makes the radiation force period doubled and phase shifted relative to the pressure wave $p_a \cos(kz)$. Note that Φ is positive (negative) if the density ratio $(5\tilde{\rho} - 2)/(2\tilde{\rho} + 1)$ is bigger (smaller) than the compressibility ratio $\tilde{\kappa}$. This sign-difference was used by the Laurrell group in its seminal work from 2004 on acoustophoretic separation of red blood cells and lipid particles.⁶⁻⁸ A sketch of the acoustic radiation force is shown in Fig. 2.

Most of the parameters needed as input for theoretical calculations can easily be estimated from table values of materials and from the geometry of the given acoustofluidic device. However, the energy density is not so easy to estimate, since the coupling of acoustic energy from the piezo transducer into the fluidic system is hard to predict as discussed in Part 3 and 4 of the Tutorial Series.^{9,10} A typical value for low-voltage (≤ 10 V) piezo transducers running at a few MHz on silicon/glass chips is¹¹⁻¹⁴

$$E_{\text{ac}} \approx 10\text{--}100 \text{ Jm}^{-3}. \quad (31)$$

In the following, we present experimental validation of the above theory of the acoustic radiation force.

V. Acoustophoretic particle tracks

Basic physical properties of acoustophoresis, such as energy density, local pressure amplitudes, acoustophoretic velocity fields, resonance line shapes, and resonance Q factors, are most easily studied in simple rectangular channels embedded in silicon/glass chips like those described in Part 5 of the Tutorial Series.¹⁵ Examples of this approach are given in refs. 13 and 14. In both of these papers, the microfluidic chips under study contain a straight channel with one inlet and one outlet. Typical dimensions of the channels are length $l = 40$ mm, width $w = 0.38$ mm, and height $h = 0.16$ mm. The particles were liquid suspensions of 5 μm -diameter polystyrene microbeads in concentrations ranging from 0.1 g L^{-1} to 0.5 g L^{-1} . The ultrasound frequency is around 2 MHz corresponding to λ around 0.75 mm ensuring the validity of the basic assumption $a \ll \lambda$ of the theory.

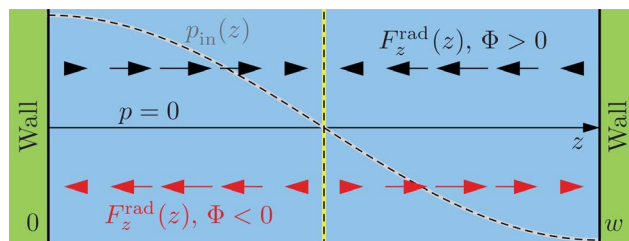


Fig. 2 A cross-sectional sketch of a straight, hard-walled (green) water-filled channel (blue) of width w with a transverse, standing, ultrasound $\lambda/2$ -pressure resonance $p_{\text{in}}(z) = p_a \cos(kz)$ (gray dashed line), $k = \pi/w$. Relative to $p_{\text{in}}(z)$, the radiation force $F_z^{\text{rad}}(z)$ on a small suspended particle is period doubled and phase shifted. For a contrast factor $\Phi > 0$ we have $F_z^{\text{rad}}(z) \propto \sin(2kz)$ (black arrows), and for $\Phi < 0$ we have $F_z^{\text{rad}}(z) \propto -\sin(2kz)$ (red arrows). Consequently, the resulting particle motion is towards and away from the nodal plane (yellow dashed line), respectively.

In Part 2 of the Tutorial Series⁵ we have already reviewed the determination of the acoustic resonance properties in ref. 13, such as the Q factor and the resonance width. Here we will illustrate the experimental validation of the above theory by briefly reviewing the study of the acoustophoretic particle tracks in refs. 13 and 14.

Assuming the channel is aligned with the x -axis and the ultrasonic standing wave is applied in the transverse z -direction, the path of a microbead moving by acoustophoresis is traced out by the time-dependent co-ordinates $(x(t), z(t))$. A particularly simple analytical expression for the transverse part, $z(t)$, of such a path can be obtained from the acoustic radiation force eqn (30a), valid for the 1D planar standing $\lambda/2$ -wave $p_1(z, t)$, eqn (28b). For slowly moving micrometre-sized particles we can safely neglect inertial effects and determine the transverse path, $z(t)$, by balancing the acoustophoretic force F_z^{rad} with the viscous Stokes drag force, $F_z^{\text{drag}} = -6\pi\eta a v_p$, from the quiescent liquid. This force balance results in an expression for the position-dependent particle speed v_p ,

$$v_p(z) = \frac{2\pi\Phi k a^2 E_{\text{ac}}}{3\pi\eta} \sin(2kz). \quad (32)$$

Writing $v_p = dz/dt$, the resulting differential equation for the transverse particle path $z(t)$ can be solved analytically by separation in the variables z and t , and using the integral $2 \int ds/\sin(2s) = \ln|\tan(s)|$,

$$z(t) = \frac{1}{k} \arctan \left\{ \tan[kz(0)] \times \exp \left[\frac{4\Phi}{3} (ka)^2 \frac{E_{\text{ac}} t}{\eta} \right] \right\}, \quad (33)$$

where $z(0)$ is the transverse position at time $t = 0$. In Fig. 3(a) is shown the experimental validation of eqn (33) from ref. 14. The blue points are data for actual particle paths determined by particle tracking frame by frame from a recorded CCD video of the particle motion. The black lines are fitted to data using eqn (33) with only one fitting parameter, the acoustic energy density E_{ac} . The average of the determination of E_{ac} for 100 particle tracks by this method resulted in $E_{ac} = (103 \pm 12) \text{ J m}^{-3}$.

In Fig. 3(b) are shown micro-particle image velocimetry (micro-PIV) measurements of the transverse acoustophoretic velocity $v_p(z)$. For a microscope field-of-view covering a 0.85-mm-long segment of the 0.38-mm-wide channel, the data are obtained from the first image-pair in 100 repeated experiments of acoustophoretic focusing each starting from a homogeneous particle distribution. After averaging along the channel length, the data are fitted to the acoustophoretic particle velocity $v_p(z)$ of eqn (32) with E_{ac} as the only fitting parameter. The resulting value of $E_{ac} = (98.0 \pm 1.1) \text{ J m}^{-3}$ is in excellent agreement with, and more precise than, the particle tracking method. These results provide a good validation of the theory.

Inverting the expression, we can also calculate the time t it takes a particle to move from any initial position $z(0)$ to any final position $z(t)$,

$$t = \frac{3\eta}{4\Phi(ka^2)E_{ac}} \ln \left[\frac{\tan[kz(t)]}{\tan[kz(0)]} \right] \quad (34)$$

$$= \frac{3}{4\Phi} \frac{c_0^2}{\omega^2 a^2} \frac{\eta}{E_{ac}} \ln \left[\frac{\tan[kz(t)]}{\tan[kz(0)]} \right].$$

This expression is important for designing acoustofluidic devices to separate particles having the same sign of their acoustophoretic contrast factor Φ . In this case separation must be based on variations in the time $t(w)$ it takes a particle to be focused transversely given the width w of the microfluidic channel. If the axial convection speed of the carrier liquid is v_0 , then the distance $\Delta l(v_0, w)$ a given particle has to flow along the channel before it has moved the transverse focus distance w can be written as

$$\Delta l(v_0, w) = v_0 t(w) \propto a^{-2} \Phi^{-1} v_0 \omega^{-2} E_{ac}^{-1}. \quad (35)$$

The larger a particle, the shorter it has to be convected before it has been focused. An analysis of the

acoustophoretic focus time in terms of the focusing ability is provided in ref. 14.

VI. Energy density as function of the applied piezo voltage

In Part 4 of the Tutorial Series,¹⁰ the basic theory of piezoelectric actuation of ultrasonic resonances in water-filled silicon/glass microchannels is presented. It is shown that a linear relation exists between the applied peak-to-peak voltage U_{pp} of the piezo transducer responsible for exciting the ultrasonic resonance and the induced acoustic pressure amplitude p_a ,

$$p_a \propto U_{pp}. \quad (36)$$

By eqn (30b) E_{ac} thus scales with the square of U_{pp} ,

$$E_{ac} \propto p_a^2 \propto U_{pp}^2. \quad (37)$$

This scaling law was tested in ref. 13 by plotting the values of E_{ac} extracted by the above-mentioned particle-tracking method versus the applied piezo-transducer voltage U_{pp} . The result is shown in Fig. 4 for ten values of U_{pp} in the range 0.4 V to 1.9 V. A power-law fit resulted in the power 2.07, less than 5% from the expected power of 2.

The measurements of the acoustic energy density E_{ac} also allows for a determination of the pressure amplitude p_a . For water at room temperature we obtain from eqn (30b) that

$$p_a = 2\sqrt{\rho_0 c_0^2 E_{ac}} = 0.094 \text{ MPa} \sqrt{\frac{E_{ac}}{1 \text{ J m}^{-3}}}. \quad (38)$$

For the energy density $E_{ac} \approx 100 \text{ J m}^{-3}$, obtained in Fig. 3, we find $p_a \approx 1 \text{ MPa}$ or 4×10^{-4} times the cohesive energy density 2.6 GPa of water. Equivalently, the density fluctuations are 4×10^{-4} times ρ_0 ,

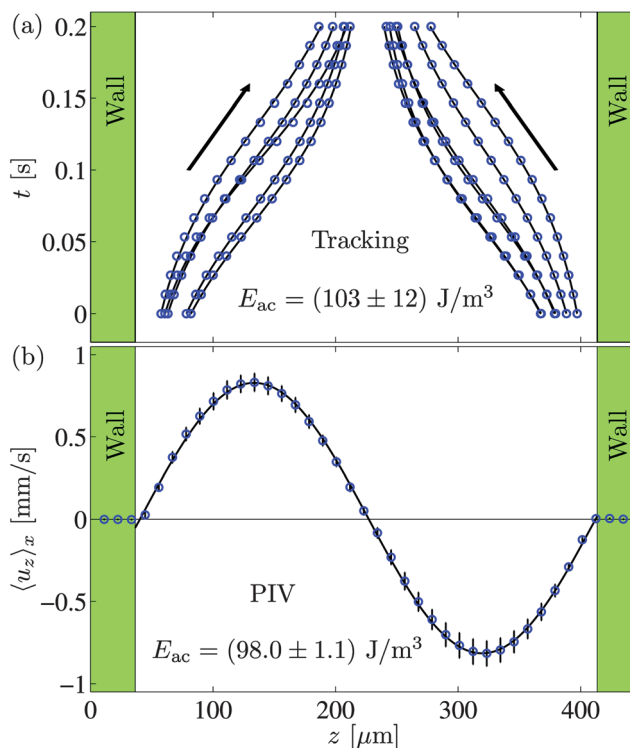


Fig. 3 Experimental validation of the theory of the acoustic radiation force for 5 μm -diameter polystyrene particles in water ($\bar{\kappa} = 0.72$, $\bar{\rho} = 1.05$, and $\Phi = 0.11$) in a 1D planar standing $\lambda/2$ -pressure wave. (a) Plot of the transverse path $z(t)$ (blue circles) and corresponding fitting lines eqn (33) (black lines) for 16 out of 100 measured particle tracks. For each fit, E_{ac} is the only fitting parameter. The average of all fits resulted in $E_{ac} = (103 \pm 12) \text{ J m}^{-3}$. (b) Plot of the average $\langle u_z \rangle_x$ (blue circles) along the channel of the z -component of the particle velocity measured by micro-PIV. The data are obtained from the first image-pair in 100 repeated experiments of acoustophoretic focusing, each starting from a homogeneous particle distribution. The acoustophoretic particle velocity v_p of eqn (32) is fitted to data with E_{ac} as the only fitting parameter resulting in $E_{ac} = (98.0 \pm 1.1) \text{ J m}^{-3}$. Adapted from ref. 14.

and thus the acoustic perturbation theory is expected to hold even at resonance.

VII. Viscous corrections to the radiation force

The theory of the acoustic radiation force has so far been developed under the assumption of an inviscid fluid. Going back to the perturbation theory reviewed in Part 2 of the Tutorial Series,⁵ this amounts to neglecting the viscous term $\eta \nabla^2 v_1$ relative to $\rho_0 \partial_t v_1$ in the Navier–Stokes equation. Far from any rigid boundaries, this is a good approximation. However, the bulk velocity oscillating at an ultrasound frequency, ω , must match the no-slip boundary condition at any given rigid wall, and it is well known by momentum diffusion considerations^{16,17} that during one oscillation period, the presence of a wall can be felt up to the penetration depth δ , given in terms of the kinematic viscosity $\nu = \eta/\rho_0$ as,

$$\delta = \sqrt{\frac{2\nu}{\omega}} \approx 0.6 \mu\text{m}, \quad (39)$$

where the value is for 1 MHz ultrasound in water at room temperature. For distances within a few times δ , large velocity gradients may occur in eqn (2b), such that $\eta v_1/\delta^2 \gtrsim \rho_0 \partial_t v_1$, and viscosity cannot be neglected. This viscous fluid layer surrounding a given particle is referred to as the acoustic boundary layer. For a particle radius $a \gg \delta$ the boundary layer is of negligible relative size, and the inviscid theory is expected to be a good approximation.

In previous works by Doinikov¹⁸ and by Danilov and Mironov,¹⁹ general theoretical schemes for the radiation force have been developed, but analytical expressions were only provided in the special limits of $a \ll \delta \ll \lambda$ and $\delta \ll a \ll \lambda$. Given the magnitude of δ above, the range of applicability of these published expressions for viscous corrections is severely limited. In recent work by Settles and Bruus,^{20,21} an analytical expression for the radiation force was derived for any (small) particle size $\delta, a \ll \lambda$ using the classic Prandtl–Schlichting boundary-layer theory combined with a stream-function formulation of the acoustic boundary layer.¹⁷ The inviscid bulk field is coupled to the motion of the particle through the boundary layer, and not directly as in eqn (21) above.

The result of the analysis of ref. 21 is that the monopole scattering coefficient f_1 is unchanged (the mass scattering and the compressibility are unaffected by viscosity), while f_2 becomes complex-valued,

$$f_2(\tilde{\rho}, \tilde{\delta}) = \frac{2[1 - \gamma(\tilde{\delta})](\tilde{\rho} - 1)}{2\tilde{\rho} + 1 - 3\gamma(\tilde{\delta})}, \quad (40a)$$

$$\gamma(\tilde{\delta}) = -\frac{3}{2}[1 + i(1 + \tilde{\delta})]\tilde{\delta},$$

with $\tilde{\delta} = \frac{\delta}{a}$. (40b)

The viscosity-dependent correction to the final expression (27) consists in replacing $f_2(\tilde{\rho})$ by $\text{Re}[f_2(\tilde{\rho}, \tilde{\delta})]$. In the inviscid case $\tilde{\delta} = 0$, we find that $f_2(\tilde{\rho}, \tilde{\delta} = 0) = f_2(\tilde{\rho})$, as expected, and for neutral-buoyancy particles ($\tilde{\rho} = 1$) f_2 is identically zero. As a function of decreasing particle radius a , the value of $f_2(\tilde{\rho}, \tilde{\delta})$ saturates asymptotically, and $f_2(\tilde{\rho}, \tilde{\delta} \gg 1) = (2/3)(\tilde{\rho} - 1)$.

Using tabulated values of the material parameters, it is found that the relative change in the acoustic contrast factor Φ is about 1% or less for 5 μm -diameter, near-neutral buoyancy, polystyrene particles in water, but as much as 25% for pyrex glass particles with a diameter of 0.5 μm .²¹

VIII. Concluding remarks

In this Tutorial Paper we have used first-order and time-averaged second-order perturbation theory to derive an expression for the acoustic radiation force F^{rad} at wavelength λ for a small spherical particle of radius a in an inviscid fluid.

The expression is the sum of the monopole term for a compressible, stationary particle with coefficient f_1 , which depends only on the relative compressibility $\tilde{\kappa}$, and the dipole term for a moving, incompressible particle with coefficient f_2 , which depends only on the relative density $\tilde{\rho}$. Examples of experimental validation of the theory have been presented, and a brief review of how the inclusion of the fluid viscosity alters the result. Viscosity plays no role for near-neutral buoyancy particles, while significant corrections appear for particles with a density differing greatly from water. A more detailed treatment of the acoustic boundary layer is given in the coming parts of Tutorial Series treating acoustic streaming.

In this tutorial paper, we have not discussed size effects for particles with radius a comparable to or larger than the acoustic wavelength λ . A good entry to such studies is the theoretical analysis by Hasegawa.²²

Another aspect not touched upon here, and which also needs more studies is particle–particle interactions. We have only studied the single-particle theory. However, at least two effects play a role as the concentration of the suspended particles is increased. One is hydrodynamic interaction, where one particle feels the Stokes drag from the wake produced by the motion of another particle. A very good and general introduction is given in the textbook by Happel and Brenner,²³ while an explicit example of many-particle effects in microchannel magnetophoresis as function of concentration is given in ref. 24.

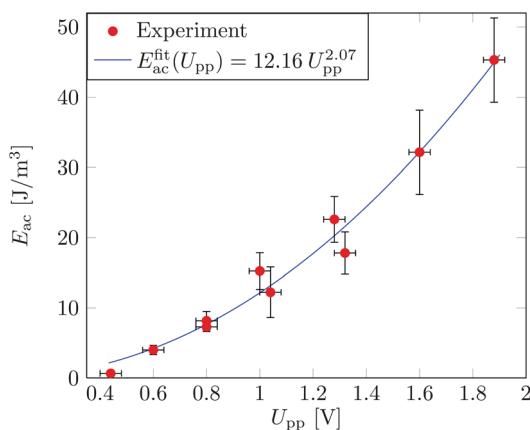


Fig. 4 Measured acoustic energy density E_{ac} versus applied peak-to-peak voltage U_{pp} on the piezo transducer (points) using the particle-tracking method on 5 μm -diameter polystyrene particles in water. The power law fit (full line) to the data is close to the expected square law, $E_{ac} \propto U_{pp}^2$. Adapted from ref. 13.

In the coming years we will likely see more work on acoustofluidics²⁵ and high particle concentration acoustophoresis and its application to biomedical samples.

Acknowledgements

This work was supported by the Danish Council for Independent Research, Technology and Production Sciences, Grant No. 274-09-0342.

References

- 1 H. Bruus, *Lab Chip*, 2011, **11**, 3742–3751.
- 2 L. V. King, *Proc. R. Soc. London, Ser. A*, 1934, **147**, 212–240.
- 3 K. Yosioka and Y. Kawasima, *Acustica*, 1955, **5**, 167–173.
- 4 L. P. Gorkov, *Soviet Physics - Doklady*, 1962, **6**, 773–775.
- 5 H. Bruus, *Lab Chip*, 2012, **12**, 20–28.
- 6 H. Jonsson, C. Holm, A. Nilsson, F. Petersson, P. Johnsson and T. Laurell, *Ann. Thorac. Surg.*, 2004, **78**, 1572–1578.
- 7 F. Petersson, A. Nilsson, C. Holm, H. Jönsson and T. Laurell, *Analyst*, 2004, **129**, 938–43.
- 8 F. Petersson, A. Nilsson, C. Holm, H. Jönsson and T. Laurell, *Lab Chip*, 2005, **5**, 20–2.
- 9 J. Dual and T. Schwarz, *Lab Chip*, 2012, **12**, 244–252.
- 10 J. Dual and D. Möller, *Lab Chip*, 2012, **12**, 506–514.
- 11 M. Wiklund, P. Spéjel, S. Nilsson and H. M. Hertz, *Ultrasonics*, 2003, **41**, 329–333.
- 12 J. Hultström, O. Manneberg, K. Dopf, H. M. Hertz, H. Brismar and M. Wiklund, *Ultrasound Med. Biol.*, 2007, **33**, 145–151.
- 13 R. Barnkob, P. Augustsson, T. Laurell and H. Bruus, *Lab Chip*, 2010, **10**, 563–570.
- 14 P. Augustsson, R. Barnkob, S. T. Wereley, H. Bruus and T. Laurell, *Lab Chip*, 2011, **11**, 4152–4164.
- 15 A. Lenshof, M. Evander, T. Laurell and J. Nilsson, *Lab Chip*, 2012, **12**, 684–695.
- 16 L. Rayleigh, *Philos. Trans. R. Soc. London*, 1884, **175**, 1–21.
- 17 L. D. Landau and E. M. Lifshitz, *Fluid Mechanics*, Pergamon Press, Oxford, 2nd edn, 1993, vol. 6, Course of Theoretical Physics.
- 18 A. Doinikov, *J. Acoust. Soc. Am.*, 1997, **101**, 722–730.
- 19 S. Danilov and M. Mironov, *J. Acoust. Soc. Am.*, 2000, **107**, 143–153.
- 20 M. Settnes and H. Bruus, *Proc. 15th MicroTAS, 2–6 October 2011*, Seattle (WA), USA, 2011, pp. 160–162.
- 21 M. Settnes and H. Bruus, *Phys Rev E*, 2012, **85**, 016327.
- 22 T. Hasegawa, *J. Acoust. Soc. Am.*, 1977, **61**, 1445–1448.
- 23 J. Happel and H. Brenner, *Low Reynolds number hydrodynamics with special applications to particulate media*, Martinus Nijhoff Publishers, The Hague, 1983.
- 24 C. Mikkelsen and H. Bruus, *Lab Chip*, 2005, **5**, 1293–1297.
- 25 J. Friend and L. Y. Yeo, *Rev. Mod. Phys.*, 2011, **83**, 647–704.